RSC Advances

ROYAL SOCIETY OF CHEMISTRY

www.rsc.org/advances

Cite this: DOI: 10.1039/c0xx00000x

www.rsc.org/xxxxxx

ARTICLE TYPE

Probing the structural and electronic properties in silicon-based clusters: MSi_6^- and MSi_6 (M=La, Ce, Yb and Lu)

Huai-Qian Wang* and Hui-Fang Li

Received (in XXX, XXX) Xth XXXXXXXXX 20XX, Accepted Xth XXXXXXXXX 20XX

DOI: 10.1039/b000000x

The neutral and charged silicon clusters Si_6^q (q=0, –1) are doped systematically with an external atom of different lanthanides: La, Ce, Yb and Lu. The structural, electronic, and magnetic properties of the doped clusters, MSi_6^q (M=La, Ce, Yb and Lu; q=0, –1) are investigated using the Saunders "Kick" global stochastic search technique combined with density functional theory (DFT) calculations. The accuracy and consistency of structure optimization of MSi_6^q clusters are tested with three exchange correlation functional (PBEPBE, BPW91 and B3LYP). DFT calculations show that the pentagonal bipyramid structures of MSi_6^- (M=Yb, Lu) and $Si_{6/7}^-$ with high symmetry are ground state structures, which give simulated photoelectron spectra in good agreement with available experiments. The detailed comparison between previously published experimental photoelectron spectra and the present theoretical simulation helps to identify the ground state structures. The neutral species show the impurity as a four-coordinate atom in the equatorial plane of pentagonal bipyramid. Furthermore, the current magnetic property analysis indicates that the magnetic moment of the doped rare earth atoms remain largely localized and the atomiclike magnetism is maintained in the doped clusters.

1. Introduction

Since silicon is the keystone of modern semiconductor technology, it attracts great attention as building blocks for silicon-based nanomaterials. Silicon clusters have been the subject of extensive experimental[1–6] and theoretical[7–12] studies in the past two decades. It was observed that these clusters tend to form compact, diamond-like structures rather than the fullerene-like cages that are characteristic of their congener, carbon.[13] These results are ascribed to the fact that silicon atoms much prefer sp^3 hybridization to sp^2. The doping of a suitable metal atom into a pure Si cluster, a highly stabilized cluster will open up a new avenue to cluster-assembled materials made from Si atoms. More significantly, however, the lion's share of that interest stems from the realization that the addition of "impurity" atoms can significantly alter the properties of silicon. For example, the notion of altering the electronic properties of silicon by doping group IIIA (Ga, Al) and group VA (P, As) elements into it has been in use for over half a century and has led to the revolutionary rise of modern computers. As we know, the first hints that silicon cages may be stabilized by the introduction of a doping atom emerged from the early, pioneering experimental work of Beck who observed enhanced ion intensities of metal-silicon clusters, MSi_n^+ (M=Mo, Cr, W), around n=16 when a transition metal atom was added to the cluster.[14] Since then, many stable MSi_n species have been reported in which various factors accounting for their formation have been examined experimentally[15–23] and theoretically.[24–34] Recently, infrared multiple photon dissociation (IR-MPD) and mass spectrometry are used to identify the structures of small neutral vanadium and manganese doped silicon clusters Si_nX (n = 6–9, X=V and Mn).[15] Recent theoretical work on doping silicon anion clusters with yttrium suggests that the two important growth behaviors have been found: (1) the metal atom acts as a linker between two subclusters and (2) the metal atom is endohedrally encapsulated in a silicon cage.[25]

The rare earths (RE) are special transition metals, possessing many of properties (such as optical property, magnetism) as these transition elements do. RE compounds are usually used as catalysts, and synthetic products in the production of petroleum. Up to now, only a few reports exist on RE-doped silicon clusters.[17,25,29,35–37] However, interest in their potential applications spurred considerable activity over the past couple of years. We have recently published the results of comparing experimental photoelectron spectroscopy and theoretical density functional theory (DFT) studies of $MSi_6^{-/0}$ (M = Pr, Gd, Ho) clusters.[35] This article provides an interesting example for evaluating the accuracies of various DFT methods, in general, verify the proposed structural types for these species. Experimentally, the validity of the concept can be proved by using photoelectron spectroscopy, which is shown to be a powerful experimental technique for probing electronic structures of size-selected clusters.[38–45] Especially, Bowen and co-workers have investigated the lanthanide-silicon cluster anions $LnSi_n^-$ ($3 \le n \le 13$; Ln= Ho, Gd, Pr, Sm, Eu, Yb)[46] and $EuSi_n^-$ ($3 \le n \le 17$)[17] by using photoelectron spectroscopy method. They proposed that the building blocks of silicon-based cluster may exist as magnetic materials. They also proposed that the Eu atom encapsulated into the Si_n clusters at the size n=12, which has been convinced by

theoretical calculation.[29] In addition, Nakajima and co-workers have previously reported the electronic properties of silicon clusters containing a transition or lanthanide metal atom from group 3, 4, or 5 by using anion photoelectron spectroscopy at 213 nm.[47]

Here, we report the generation of a series of anionic and neutral lanthanide-metal-doped silicon clusters MSi_6 (M= La, Ce, Yb and Lu) using Saunders "Kick" global stochastic search technique combined with DFT geometric optimization. The aim of the present work is: (1) to obtain the various global minimum structures of MSi_6^q clusters; (2) to compare the results of our extensive computations with previously experimental findings.[46, 47] Good agreement between previously measured photoelectron spectroscopy and theoretical simulations helps to identify the ground states of the anionic and neutral RE-doped MSi_6 clusters. The rest of this article is organized as follows: We describe our computational details and theoretical backgrounds in Section 2; Section 3 "Results and discussions" introduces and compares various geometric structures, simulated photoelectron spectra (PES), electronic and magnetic properties; finally, the "Conclusions" is given in the last Section.

2. Computational methods

The calculations in this work began with unbiased searches for the low-lying structures of a series of anionic and neutral RE-doped silicon clusters MSi_6 (M= La, Ce, Yb and Lu) by using the Saunders "Kick" (SK) global search technique[48] combined with DFT geometric optimization (SK-DFT) within the generalized gradient approximation in the Perdue–Burke–Ernzerhof (PBE)[49] functional form using the GAUSSIAN09 program.[50] This SK stochastic method generates structures randomly and facilitates the thorough exploration of unknown isomers much more easily than manual methods. Specifically, all the atoms are placed at the same point initially and then are "kicked" randomly within a sphere of radius R (R is the maximum kick distance), *e.g.*, a hollow sphere of inside radius 10 Å. The method developed further in this work generates up to 500 unbiased starting geometries and then submits them automatically for optimization with GAUSSIAN09. We recently have successfully employed the SK-DFT method for global minimum searches on a series of bimetallic cluster and vanadium oxides.[51–57] The scheme of this research consists of the following four steps. Firstly, the initial SK global minimum search was performed using the DFT method known in the literature as "PBEPBE" functional[49] with a scalar relativistic effective core potential and LANL2DZ basis set for RE atom and 6–31G basis set for Si atom (the PBEPBE/RE/LANL2DZ/Si/6–31G level) implemented in the GAUSSIAN09 package. Many structural isomers were generated for each cluster. The kick method runs at the PBEPBE/RE/LANL2DZ/Si/6–31G level some 500 times until no new minima appeared. If this procedure is repeated enough times, eventually all isomeric structures for the cluster will be found. Secondly, the distinct isomers were ranked according to their relative energies at the PBEPBE/RE/LANL2DZ/Si/6–31G level. Meanwhile, the effect of spin multiplicity is also taken into account in the present study. Thirdly, we selected the top-8 lowest-energy isomers for each species, those with their energy value within ~1.50 eV from the lowest-energy isomer are to be further optimized using the PBE PBE exchange-correlation functional with the larger RE/SDD/Si/6–311+G(d) basis sets (the PBEPBE/RE/SDD/Si/6–311+G(d) level). Here, the SDD basis set[58] along with the quasi-relativistic MWB (28 core electrons) pseudopotential,[58,59] was chosen for RE atoms. For transition metals compounds, lanthanides and actinides the SDD basis set is standard practice, it is slightly superior and usually gives very nice structures.[60] For Si atom, we adopted the 6–311+G(d) basis set. Such diffuse functions improve the predicted properties of species with extended electronic densities such as anions. Finally, the top-several isomers were ranked again by their relative energies at high PBE PBE/RE/SDD/Si/6–311+G(d) level, those with their energy value within 0.40 eV from the lowest-energy isomer were all regarded as potential candidate lowest-energy structures. All the optimazation procedure was carried without any symmetry constraint. This was followed by frequency calculations to assure that all found structures are at local minima of the potential energy surface and have real frequencies.

The reliability of the present computational method (at PBE PBE/RE/SDD/Si/6–311+G(d) level) was validated by performing calculations on the features of simulated PES spectra and the first adiabatic/vertical detachment energy (ADE/VDE) for which experimental results are available (see Figs. 2, 5, 6; Table 3).[4,6,46,47] Furthermore, geometry optimization of MSi_6 (M= La, Ce, Yb and Lu) clusters were tested with several exchange-correlation functionals (PBEPBE,[49] BPW91[61,62] and B3LYP[63–65]) for accuracy and consistency. The calculated results using these three different DFT levels are presented in Table 2. These results underline that the geometries of all the clusters obtained by three functionals are similar, although the order of isomers is reversed in some cases. Here, only PBEPBE results will be discussed in the text. In addition, due to the possible multireference structure of wavefunction, the DFT functional we employed here may be insufficient in giving very accurate description. The multi-reference configuration interaction (MRCI) method, which is based on multiconfiguration self-consistent field (MC-SCF) wavefunction would be more optimal for present clusters. Unfortunately, it is currently not computationally feasible to study the RE-doped clusters using this advanced theoretical method. Geometries are regarded as optimized when the maximum force, the root-mean-square (RMS) force, the maximum displacement of atoms, and the RMS displacement of atoms have magnitudes less than 0.00045, 0.0003, 0.0018, and 0.0012 a.u., respectively. Because the computed zero-point energy (ZPE) corrections of the isomers of a specific cluster size are small and almost the same, they are not expected to affect the relative energy ordering. Hence, the relative energies of isomers are obtained from the total electronic energies (excluding ZPE).

We used three criteria in comparing the theoretical results with the experimental data to select our most likely candidate structures: (1) the relative energies; (2) the first VDE and ADE; (3) the number of distinct peaks of simulated PES in the low binding energy range of ≤ 266 nm (4.661 eV) and their relative positions. The first criterion addresses typical errors in DFT calculations, which is about several tenth of an electron volt in relative energies for MSi_6^q clusters. In the present study, we used a cutoff energy of 0.40 eV at the PBEPBE/RE/SDD/Si/6–311+G(d) level to collect low-lying isomers. Next, we calculated the

first VDE (which is defined as the energy difference between the neutral clusters at optimized anion geometry clusters and optimized anion clusters: VDE=$E_{\text{neutral at optimized anion geometry}} - E_{\text{optimized anion}}$) and ADE (which is the energy difference between the optimized anion geometry and the optimized neutral geometry: ADE=$E_{\text{optimized neutral}} - E_{\text{optimized anion}}$). Finally, the simulated spectra were then compared to the measured PES spectra to distinguish from top candidates for the low-lying isomers. VDEs were calculated using the generalized Koopmans' theorem by adding a correction term to the eigenvalues of the anion.[66] The correction term was calculated as $\delta E=E_1\text{-}E_2\text{-}\varepsilon_{\text{HOMO}}$, where E_1 and E_2 are the total energies of the anion and neutral, respectively, in their ground states at the anion equilibrium geometry and $\varepsilon_{\text{HOMO}}$ corresponds to the eigenvalue of the highest occupied molecular orbital (HOMO) of the anion. The simulated PES spectra were fitted with a full width at half-maximum (FWHM) of 0.20 eV.[53] The methods have been used successfully in a number of previous studies and have been shown to yield VDEs in good agreement with PES data.[38–45] We paid particular attention to the number of peaks below 4.661 eV. Only those isomers that meet all three criteria are considered to be the superlative candidates for MSi_6^- clusters.

Table 1 Various structures with the symmetry type (Sym), the spin multiplicity (SM), the binding energy (BE) per atom, the doping energy (DE) per atom, HOMO-LUMO energy gap E_{gap}, and energy separation of the isomeric structures from the lowest-energy structures (ΔE) of both pure $Si_{6/7}^q$ (q=0, –1) clusters and MSi_6^q (M=La, Ce, Yb and Lu; q=0, –1) clusters.

Cluster	The lowest-energy isomer						Low lying isomer			
	Isomer	SM	Sym	BE (eV)	DE (eV)	E_{gap} (eV)	Isomer	E(eV)	Isomer	E(eV)
Si_6	*c*	1	C_{2v}	3.42		2.15	*d*	0.62	*e*	1.45
Si_6^-	*a*	2	C_{2v}	3.55		0.55	*b*	0.19	*d*	0.85
Si_7	*f*	1	D_{5h}	3.56	4.37	2.12	*g*	0.96	*h*	0.97
Si_7^-	*f*	2	D_{5h}	3.62	4.04	0.59	*g*	0.79	*h*	0.87
$LaSi_6$	*i*	2	C_1	3.59	4.59	0.32	*m*	0.29	*k*	0.30
$LaSi_6^-$	*j*	1	C_{5v}	3.82	4.45	1.04	*k*	0.29	*l*	0.34
$CeSi_6$	*i*	3	C_s	5.35	16.93	0.17	*l*	0.39	*k*	0.42
$CeSi_6^-$	*j*	2	C_s	5.63	16.73	0.49	*k*	0.34	*l*	0.37
$YbSi_6$	*i*	1	C_{2v}	3.16	1.58	0.62	*o*	0.71	*p*	0.84
$YbSi_6^-$	*i*	2	C_{2v}	3.67	1.17	0.42	*j*	0.34	*p*	0.56
$LuSi_6$	*i*	2	C_{2v}	3.35	2.90	0.68	*m*	0.47	*j*	0.51
$LuSi_6^-$	*j*	1	C_{5v}	3.81	3.01	1.36	*i*	0.35	*l*	0.53

Table 1 (Continued)

Cluster	Low lying isomer									
	Isomer	E(eV)	Isomer	E(eV)	Isomer	E(eV)	Isomer	E(eV)	Isomer	E(eV)
$LaSi_6$	*l*	0.34	*o*	0.61	*p*	0.62	*j*	0.63	*n*	0.75
$LaSi_6^-$	*m*	0.36	*n*	0.65	*o*	0.72	*i*	0.82	*p*	1.44
$CeSi_6$	*m*	0.48	*j*	0.62	*o*	0.75	*n*	0.86	*p*	0.91
$CeSi_6^-$	*m*	0.38	*i*	0.62	*n*	0.71	*o*	0.86	*p*	1.35
$YbSi_6$	*j*	0.90	*l*	0.92	*n*	0.95	*m*	0.96	*k*	1.19
$YbSi_6^-$	*o*	0.63	*l*	0.75	*m*	0.76	*k*	0.83	*n*	1.02
$LuSi_6$	*l*	0.52	*k*	0.60	*m*	0.64	*n*	0.93	*o*	0.95
$LuSi_6^-$	*m*	0.53	*k*	0.63	*o*	0.79	*p*	0.95	*n*	1.02

Table 2 Relative energies in eV for selected low-lying isomers of MSi_6 (M=La, Ce, Yb and Lu) with different density functional methods.

Cluster	Isomer	Sym	PBE	B3LYP	BPW91	Cluster	Isomer	Sym	PBE	B3LYP	BPW91
$LaSi_6$	*i*	C_1	0.00	0.00	0.00	$YbSi_6$	*i*	C_{2v}	0.00	0.00	0.00
	j	C_s	0.63	0.63	0.62		*j*	C_s	0.90	0.77	0.88
	k	C_1	0.30	0.28	0.28		*k*	C_1	1.19	1.15	1.18
	l	C_1	0.34	0.32	0.34		*l*	C_1	0.92	0.55	0.92
	m	C_s	0.29	0.24	0.27		*m*	C_s	0.96	0.74	0.93
	n	C_s	0.75	0.65	0.72		*n*	C_s	0.95	0.74	0.93
	o	C_{3v}	0.61	0.51	0.56		*o*	C_3	0.71	0.48	0.65
	p	C_s	0.62	0.79	0.81		*p*	C_{2v}	0.84	0.66	0.82
$CeSi_6$	*i*	C_s	0.00	0.00	0.00	$LuSi_6$	*i*	C_{2v}	0.00	0.00	0.00
	j	C_1	0.62	0.41	0.69		*j*	C_s	0.51	0.50	0.51
	k	C_1	0.42	0.09	0.42		*k*	C_1	0.60	0.61	0.60
	l	C_s	0.39	0.22	0.40		*l*	C_s	0.52	0.47	0.51
	m	C_s	0.48	0.15	0.39		*m*	C_s	0.47	0.48	0.47
	n	C_s	0.86	0.45	0.85		*n*	C_s	0.92	0.84	0.90
	o	C_1	0.75	0.34	0.70		*o*	C_s	0.95	0.88	1.00
	p	C_s	0.91	0.70	0.87		*p*	C_s	0.64	0.52	0.83

3. Results and discussions

The optimized anion and neutral ground-state and low-lying structures at the PBEPBE/RE/SDD/Si/6–311+G(d) level are presented in Fig. 1 for both pure $Si_{6/7}^{q}$ and RE-doped MSi_6^{q} (M= La, Ce, Yb and Lu; q=0, –1) clusters. Table 1 gives various structural and energetic characteristics of parent $Si_{6/7}^{q}$ and doped MSi_6^{q} clusters. The calculated relative energies for the top-8 lowest-energy isomers of MSi_6 (M=La, Ce, Yb and Lu) with three density functional methods are presented in Table 2. The calculated first ADE and VDE of the anionic top-several isomers as well as some experiment results are given in Table 3. Natural charges populations of the lowest-energy RE-doped MSi_6^{q} (M=La, Ce, Yb and Lu; q=0, –1) clusters are listed in Table 4. Table 5 gives the magnetic moment (μ_B) of 4*f*, 5*d*, 6*s*, and 6*p* states for RE atom, total magnetic moment (μ_B) of the RE atom, and total magnetic moment of the lowest-energy RE-doped MSi_6^{q} (M=La, Ce, Yb and Lu; q=0, –1) clusters. Figs. 2~6 display the simulated PES spectra of the top-several isomers (within ~0.40 eV), along with that of experimental PES spectra for comparison. The calculated the ADEs are obtained by optimizing the geometry of the neutrals with the ground state geometries of the anions as starting points. The HOMO (SOMO for open-shell species) and the Mülliken spin density pictures of RE-doped MSi_6^{q} (M= La, Ce, Yb and Lu; q=0, –1) clusters are presented in Figs. 7~10.

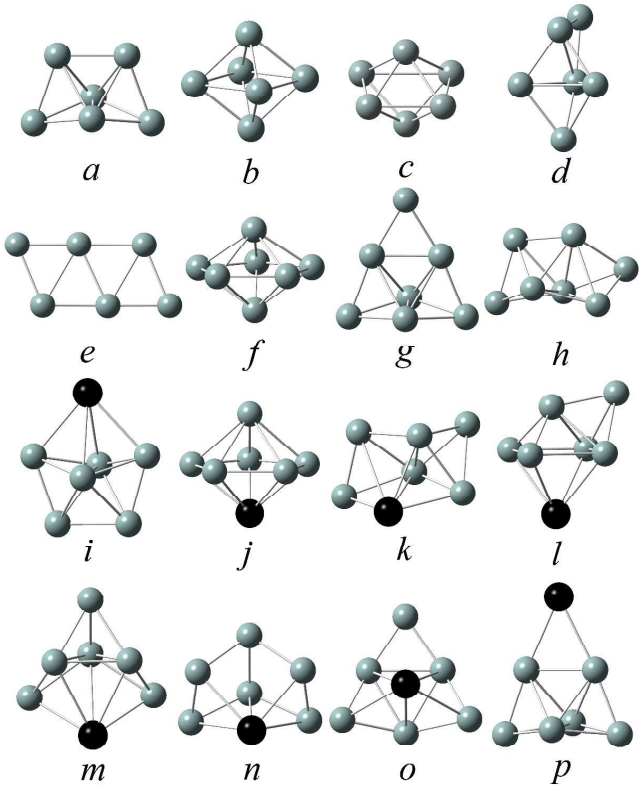

Fig. 1 Equilibrium geometries of the low-energy isomers for pure Si_6^{q} (Si_7^{q}) (q=0, –1) clusters and RE-doped MSi_6^{q} (M=La, Ce, Yb and Lu; q=0, –1) clusters at the PBEPBE/RE/SDD/Si/6–311+G(d) level of theory. The dark cyan spheres stand for silicon atoms and the black ones for RE atoms.

3.1. Geometric structure and stability

In this section we discuss the structural details of a few low-lying isomers of MSi_6^{q} clusters which were obtained by global search SK-DFT method. We have obtained many low-lying isomers and determined the lowest-energy structures for RE-doped MSi_6^{q} (M= La, Ce, Yb and Lu; q=0, –1) using the computation scheme SK-DFT described in Section 2 "Computational methods". Here, in order to discuss the effects of doped impurity atom on pure silicon clusters, we carried out an additionally SK-DFT calculation on pure $Si_{6/7}^{-,0}$ clusters. Many isomers are found and the top three isomers of $Si_{6/7}^{-,0}$ clusters are shown in Fig. 1. For Si_6^- cluster, the lowest-energy structure is isomer *a*, which can be viewed as a Si_2-capping of a bent rhombus. The point group symmetry is C_{2v}. The second lowest-energy isomer *b* is a regular octahedron with D_{4h} symmetry, and it is only 0.19 eV above the ground state. Another structure *d* obtained for Si_6^- can be formed from capping of a trigonal bipyramid. It is less stable than isomer *a* by 0.85 eV. For neutral Si_6 cluster, the lowest-energy isomer *c* is a relaxed octahedron. In fact, initial structures of isomers *a* and *b* are also considered in the present calculation. When six Si atoms were placed as the shape of isomer *a* or *b*, they move away from their original position during the geometry optimization process. The other two isomers, Si-capped triangular bipyramid-shaped isomer *d* and planar isomer *e*, are 0.62 and 1.45 eV higher than ground state structure *c*, respectively. The lowest-energy structures of Si_6^- and Si_6 are in agreement with previously reported results by using different theoretical techniques.[5,8,67] As for pure neutral and anionic Si_7 clusters, three low-lying isomers (*f*–*h*) of neutral structures are similar to the anionic structures, even the order of isomers is the same each other. The lowest-energy structure is a regular pentagonal bipyramid with D_{5h} symmetry. Our calculated structure on neutral Si_7 is in line with the early theoretical results.[3,8,12] Isomers *g* and *h* are about 0.96, 0.97 eV (for neutral Si_7) and 0.79, 0.87 eV (for anionic Si_7) less stable relative to ground state structure *f*.

The ground-state structures and some low-lying metastable isomers of RE-doped MSi_6^{q} (M= La, Ce, Yb and Lu; q=0, –1) species are shown in Fig. 1, where the dark cyan spheres stand for silicon atoms and the black ones for RE atoms. Remarkably, our calculations show that all the low-lying isomers (top-8) for MSi_6^{q} are three-dimensional (3D) structures. The spin multiplicity of ground state is kept for all other higher energy isomers (Tables 1 and 2). It must be point out that the RE atom cannot be encapsulated inside the bare Si_6^{q} cluster and still remains on the surface of the lowest-energy MSi_6^{q} cluster using three different density functional methods. The most stable structure for RE-doped MSi_6^- (M= La, Ce, and Lu), is a 3D structure with the lanthanide metal atom sitting on top (or bottom) of the regular pentagonal bipyramid (see Fig. 1, isomer *j*). These most stable structures are formed by replacing a silicon atom on the top (bottom) of inerratic pentagonal bipyramid shaped for pure Si_7 cluster. Other seven low-lying metastable 3D isomers are all much higher in energy than the perfect pentagonal bipyramid structure for all three clusters (0.29~1.44 eV for $LaSi_6^-$, 0.34~1.35 eV for $CeSi_6^-$ and 0.34~1.02 eV for $LuSi_6^-$). The M-Si

distance in the lowest-energy structures for RE-doped MSi_6^- (M= La, Ce, and Lu) has the following relationship: $R_{La\text{-}Si}$ (2.96 Å) >$R_{Ce\text{-}Si}$ (2.89 Å)>$R_{Lu\text{-}Si}$ (2.82 Å), which is mainly due to the difference in atomic radius of lanthanide-metal R_{La}=2.43 Å> R_{Ce}= 2.42 Å >R_{Lu}=2.24 Å. It should be noted that all the ground state structures of MSi_6^- (M= La, Ce, and Lu) were well retained after replacing a silicon atom on the top for pure Si_7 cluster, but electronic features had been seriously altered, which presented the reason for a far cry from photoelectron spectra. On the other hand, results for the most stable structures of the RE doped silicon clusters $YbSi_6^-$ and MSi_6 (M= La, Ce, Yb, and Lu) are also obtained. All the ground states of the neutral MSi_6 (M= La, Ce, Yb, and Lu) and $YbSi_6^-$ clusters also have a 3D structure, and no 2D isomers were obtained. The most stable structure for neutral MSi_6 (M= La, Ce, Yb, and Lu) and $YbSi_6^-$, is a 3D structure with the lanthanide metal atom sitting on side of the distorted pentagonal bipyramid (See Fig. 1, isomer *i*). For the neutral MSi_6, the high symmetry 3D pentagonal bipyramid arrangement is not a stable structure, which is much higher in energy than the most stable distorted pentagonal bipyramid by 0.63, 0.62 0.90 and 0.51 eV for the M= La, Ce, Yb, and Lu, respectively. As for $YbSi_6^-$, the structure *j* is higher than *i* by 0.34 eV. According to the above geometries describing, we find that all the lowest energy structures of neutral MSi_6 (M= La, Ce, Yb, and Lu) and $YbSi_6^-$ clusters were obtained by substituting one Si in the equatorial plane by M atom from the ground state structure (Fig. 1, isomer *f*) of $Si_7^{-,0}$ cluster, however, the anionic ground state of MSi_6 (M= La, Ce, and Lu) clusters were obtained by substituting one Si by M atom from the bottom (or top) of the pure $Si_7^{-,0}$ cluster.

It is interesting to know if the structure and stability of the clusters will be changed when an atom with full 4*f* shell is doped into Si_6 cluster compared with the case of by doping open 4*f* RE atoms. Here, we will compare the results of $YbSi_6$ and $LuSi_6$ with open 4*f* RE-doped MSi_6 (M= Ce, Pr, Eu, Gd, and Ho) clusters.[29, 35] The point group symmetry of lowest-energy structure of $YbSi_6$ and $LuSi_6$ is C_{2v} symmetry. It should be mentioned that the early RE-doped clusters MSi_6 have relatively low symmetry compared to the full 4*f* shell RE-doped clusters, e.g. $CeSi_6$ (C_s) $PrSi_6$ (C_s), $GdSi_6$ (C_s), and $HoSi_6$ (C_s). It seems that the more the *f*-electron becomes, the higher the point group symmetry is. This may be attributed to Jahn-Teller distortion. For all the RE-doped clusters MSi_6, the additional RE atom always takes one of the equatorial positions of the pentagon forming a distorted pentagonal bipyramid-shaped structure.

Table 1 gives various structural and energetic characteristics of both pure $Si_{6/7}^q$ (q=0, –1) and MSi_6^q (M=La, Ce, Yb and Lu; q=0, –1) clusters. In order to analyze the stability of Re-doped clusters, we calculated the binding energies (BE) per atom and the doping energy (DE), which are defined as the following formulas: $BE=[5E(Si)+E(Si^q)+E(M)-E(MSi_6^q)]/7$, $DE=E(Si_6^q)+E(M)-E(M\ Si_6^q)$ (M=La, Ce, Yb and Lu; q=0, –1), where $E(Si)$, $E(Si^q)$, $E(M)$, $E(MSi_6^q)$ and $E(Si_6^q)$ represent the total energies of the ground-state of Si, Si^q, RE atom M, MSi_6^q and Si_6^q clusters, respectively. The BE per atom value of the lowest-energy MSi_6^q clusters is displayed in Table 1. The notable feature is that the BE per atom in the RE-doped MSi_6^q clusters is larger than that in the pure $Si_{6/7}^q$ clusters except for the case of $YbSi_6$ and $LuSi_6$ clusters. This suggests that the Si-M bond is stronger than the Si-Si bond and the doped RE atom with open *f* shells can stabilize the pure pentagonal bipyramid structure. In fact the high stability of these clusters has been observed in $EuSi_{6/7/8}$.[29] To further study the stabilities of MSi_6^q clusters, we will discuss the DE of the ground state structure. From Table 1 we can see that both neutral and anionic $CeSi_6$ clusters have the highest DE of 16.73 and 16.93 eV among the clusters considered in present study. So, $CeSi_6^{0,-}$ should be the most stable one among these clusters. The highest occupied molecular orbital-lowest unoccupied molecular orbital (HOMO-LUMO) energy gap is another useful quantity for examining the kinetic stability of clusters. A large energy gap corresponds to a high strength required to perturb the electronic structure. To calculate the HOMO-LUMO gap we consider HOMO and LUMO of both the spins (up and down). Comparing the difference between energy gap of pure and doped clusters in Table 1 one can see that, the E_{gap} of the $LuSi_6^-$ with 1.36 eV is the largest one among the doped clusters but still smaller than the pure Si_6 and Si_7 clusters. This suggests that $LuSi_6^-$ is relatively more chemically stable than the neighboring clusters. Overall, after doping RE atom into the silicon cluster, the chemically stable of is less reactive than pure cluster.

Table 3 Experimentally measured adiabatic and vertical detachment energies (ADEs and VDEs) from the photoelectron spectra, compared to the calculated ground state or low-lying anion state ADEs and VDEs for pure $Si_{6/7}^-$ and RE-doped MSi_6 (M=La, Ce, Yb and Lu) clusters. All energies are in eV.

Cluster	Isomer	RE	ADE[a,b]	VDE[a]
Si_6^-	*a*	0.00	2.24	2.45 (2.39±0.01)[c]
	b	0.19	2.05	2.77
Si_7^-	*f*	0.00	1.91 (1.85±0.02)[d]	2.30 (2.39±0.04)[c]
	j	0.00	2.73	2.81
$LaSi_6^-$	*k*	0.29	2.11	2.18
	l	0.34	2.10	2.19
	m	0.36	2.03	2.08
$CeSi_6^-$	*j*	0.00	2.66	2.83
	k	0.34	2.12	2.19
	l	0.37	2.06	2.16
	m	0.38	2.09	2.13
$YbSi_6^-$	*i*	0.00	1.83 (1.80±0.05)[e]	1.95 (1.98)[e]
	j	0.34	2.39	2.42
$LuSi_6^-$	*j*	0.00	2.86 (2.10)[f]	3.07 (3.20)[f]
	i	0.35	2.00	2.16

[a] Numbers in parentheses represent the experimental uncertainties in the last digit. [b] Electron affinity of the neutral species. [c] From Ref. 4. [d] From Ref. 6. [e] From Ref. 46. [f] From Ref. 47.

3.2. Comparison of the PES spectrum between experiment and theory

The well-resolved PES spectra for pure $Si_{6/7}^-$ and doped MSi_6^- (M=Yb and Lu) in Fig. 2 and Figs. 5~6 at 355 nm (3.496 eV), 266 nm (4.661 eV) and 213 nm (5.83 eV) photon energy are presented by Castleman,[4] Bowen[46] and Nakajima[47] groups, respectively, it could be served as electronic fingerprints for the MSi_6^- clusters, allowing comparisons with theoretical calculations to verify the identified global minimum structures. The photoelectron spectra of present species are simulated by adding the occupied orbital energies relative to the HOMO (SOMO for open-shell systems) to the VDE and fitting them with a FWHM of 0.20 eV.[53] The simulated photoelectron spectra for the two

low-lying energy isomers of MSi_6^- (M=Yb and Lu) are presented in Figs. 5~6 for comparison. The low-lying energy isomers whose simulated spectra agree best with the experiment are assigned as the primary structure for most of the clusters. It must be pointed out that for MSi_6^- (M=La and Ce) clusters, to date no experimental PES has been reported, to facilitate the future comparison with further experiments, we have drawn the simulated PES spectra of the four lowest-lying isomers within 0.40 eV at the PBEPBE/RE/SDD/Si/6–311+G(d) level in Figs. 3~4. Furthermore, experimentally measured ADE/VDE from the anion photoelectron spectroscopy are compared with the calculated values at the PBEPBE/RE/SDD/Si/6–311+G(d) level of theory in Table 3. The calculated first ADE/VDE energies of the host clusters Si_6^- and Si_7^- are also presented in Table 3 for comparison. The VDEs of each cluster anion corresponds to the first peak maximum of each spectrum in Figs. 2~6. As shown in Table 3, the ADE/VDE are 2.73/2.81, 2.66/ 2.83, 1.83/1.95, and 2.86/3.07 eV, respectively, for M = La, Ce, Yb and Lu, which are bigger than those of $Si_{6/7}^-$ clusters (theoretical: 2.24/2.45 eV for Si_6^-, 1.91/2.30 eV for Si_7^-, experimental: the VDE is 2.39 eV for Si_6^-, 1.85±0.02/2.39 eV for Si_7^-) except for the case of $YbSi_6^-$ cluster. The calculated ADE/VDE for pure $Si_{6/7}^-$ is very in line with experimentally measured results.

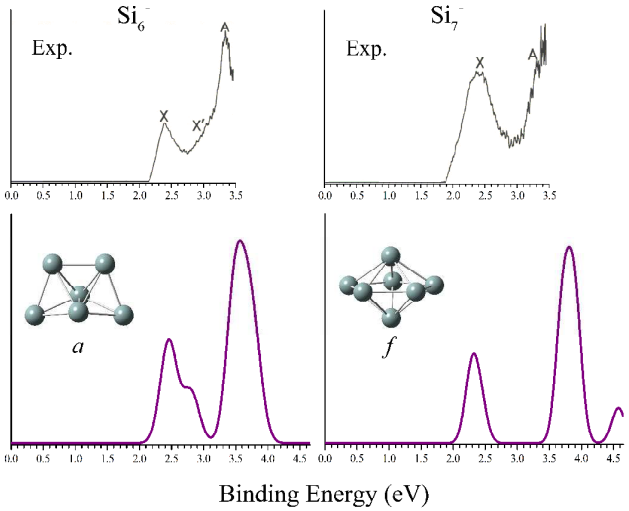

Fig. 2 Comparison of the experimental photoelectron spectra of Si_6^- and Si_7^- clusters with their simulated spectra. Each VDE was fitted with a full width at half-maximum (FWHM) of 0.20 eV to yield the simulated PES spectra. The experimental PES spectra are cited from Ref. 4.

3.2.1. Si_6^- and Si_7^-

For pure $Si_{6/7}^-$, the simulated PES spectra of the lowest-energy isomers *a* for Si_6^- and *f* for Si_7^- agree well with the experimental spectra,[4] which reproduce two prominent PES bands below 3.5 eV. The calculated first VDEs values are 2.45 and 2.30 eV, which are in agreement with the experimental values (2.39±0.01 eV for Si_6^- and 2.39±0.04 eV for Si_7^-).[4] The calculated ADE for pure Si_7^- is 1.91 eV also in line with experimentally measured result (1.85±0.02 eV).[6] For Si_6^-, the second lowest-energy isomer *b* is 0.19 eV higher in energy than *a*, considering the inherent accuracy of the DFT, we could not exclude the probability of isomer *b*. But the calculated first VDE (2.77 eV) is bigger than experimental value (2.39±0.01 eV).[4] According to the second criterion, we could exclude the possibility of the *b* isomer in the Si_6^- cluster beam. We can conclude that structures *a* and *f* should be the reasonable isomers for pure $Si_{6/7}^-$. All other structures should have been negligible contribution to the PES spectrum. The very large X-A energy gap (1.10 eV for Si_6^-, 1.50 eV for Si_7^-) between the first and second VDEs indicating that the neutral $Si_{6/7}$ clusters are closed shell singlet spin with strongest stability.

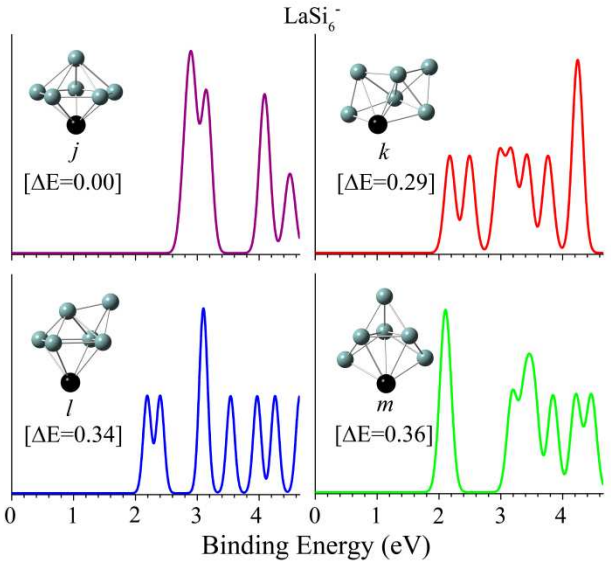

Fig. 3 Structures, relative energies, and simulated photoelectron spectra for the four low-lying isomers of $LaSi_6^-$. Each VDE was fitted with a full width at half-maximum (FWHM) of 0.20 eV to yield the simulated PES spectra.

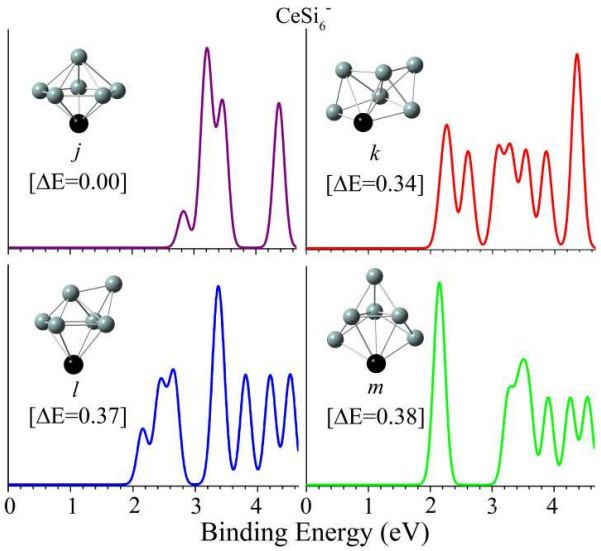

Fig. 4 Structures, relative energies, and simulated photoelectron spectra for the four low-lying isomers of $CeSi_6^-$. Each VDE was fitted with a full width at half-maximum (FWHM) of 0.20 eV to yield the simulated PES spectra.

3.2.2. $LaSi_6^-$

The ground state of $LaSi_6^-$ is closed shell (C_{5v}, ^{1}A') with a valence configuration of $(1a')^2(1a'')^2(2a')^2(3a')^2(2a'')^2(4a')^2(5a')^2(6a')^2(3a'')^2(4a'')^2(7a')^2(5a'')^2(8a')^2(9a')^2$. The first VDE corresponds to

electron detachment from the 9a' HOMO, which is an antibonding σ orbital (Fig. 7(a)). The SOMO (14a) of the neutral cluster upon removing an electron from the anion HOMO is shown in Fig. 7(b) and its spin density (Fig. 7(c)) is mainly on the La atom (0.68). As shown in Fig.3, the simulated PES patterns on the basis of the four isomers appear to be rather different, the one isomer *j* being a bit loose and consisting of four electronic states within the 0~4.661 eV, on the contrary, the others isomers (*k*, *l*, and *m*) presented more congested and consisting of six or seven electronic states. VDEs calculations for the four low-lying isomers of $LaSi_6^-$ were performed using the PBEPBE/ RE/SDD/ Si/6–311+G(d) level of theory. The lowest-energy structure *j* gives the first ADE/VDE values (2.73/2.81 eV) bigger than the pure silicon clusters (2.24/2.45 eV for Si_6^-, and 1.91/2.30 eV for Si_7^-).

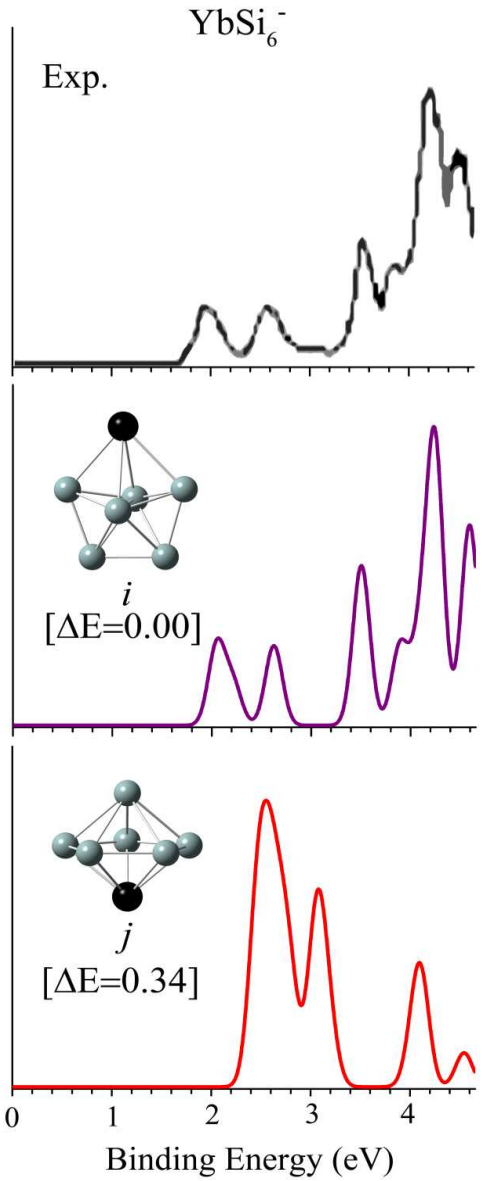

Fig. 5 Structures, relative energies, and simulated photoelectron spectra for the two low-energy isomers of $YbSi_6^-$. Each VDE was fitted with a full width at half-maximum (FWHM) of 0.20 eV to yield the simulated PES spectra. The black curve is for the experimental PES for $YbSi_6^-$. The experimental PES spectra are cited from Ref. 46.

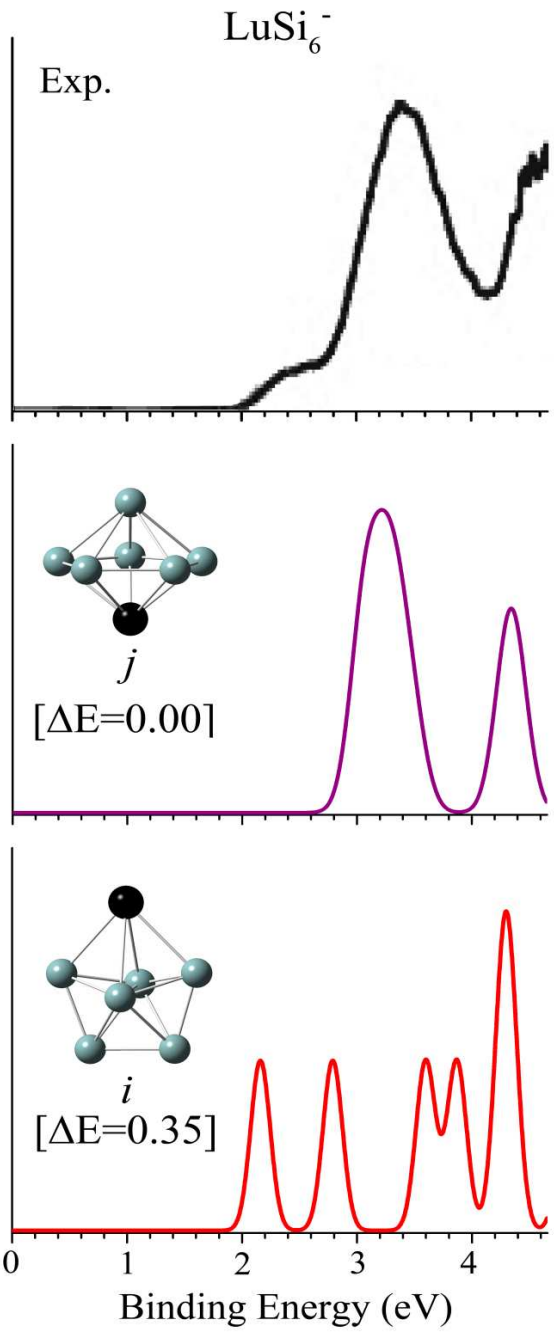

Fig. 6 Structures, relative energies, and simulated photoelectron spectra for the two low-energy isomers of $LuSi_6^-$. Each VDE was fitted with a full width at half-maximum (FWHM) of 0.20 eV to yield the simulated PES spectra. The black curve is for the experimental PES for $LuSi_6^-$. The experimental PES spectra are cited from Ref. 47.

3.2.3. $CeSi_6^-$

For $CeSi_6^-$, up to date no experimental PES spectrum has been reported, we only present our theoretical detachment spectrum from the lowest-energy and three others isomers of $CeSi_6^-$ cluster at the PBEPBE/RE/SDD/Si/6–311+G(d) level in Fig. 4. The simulated PES spectra and calculated ADE/VDE of the four low-lying isomers are presented in Fig. 4 and Table 3. The ground state of $CeSi_6^-$ is open shell (^{2}A") with a valence configuration of $(1a')^2(1a")^2(2a')^2(3a')^2(2a")^2(4a')^2(5a')^2(3a")^2(6a')^2(4a")^2(7a')^2(5a")^2(8a')^2(9a')^2(6a")^1$. The 6a" SOMO of $CeSi_6^-$ (Fig. 8(a)) is

primarily a nonbonding σ orbital. The Mülliken spin density (Fig. 8(d) and (e)) shows that the unpaired spin is primarily occupied on the Ce atom. After removal of an electron, the ground state structure of the neutral $CeSi_6$ is slightly different from $CeSi_6^-$ though it remains the C_s symmetry. The others low-lying isomers (*k*, *l*, and *m*) are found to be nearly degenerate in energy (ΔE =0.34, 0.37 and 0.38 eV) and their simulated spectra are different a lot with the ground state structure. They reproduce much more prominent PES bands than the global minimum structure *j*. The first calculated VDE (2.83 eV), corresponding to the electron detachment from the 6a" SOMO is larger than three others isomers (2.18 eV for *k*, 2.19 eV for *l* and 2.08 eV for *m*, Table 3). Detachment from the fully occupied MOs below the 6a" SOMO can lead to both singlet (S) and triplet (T) final states. At the PBEPBE level, the calculated VDEs from the $(9a')^2$ (T, S), $(8a')^2$ (T, S), and $(5a'')^2$ (T, S) orbitals are corresponding to the intense and broad A band (ranging from 3.14 to 3.25 eV).

3.2.4. $YbSi_6^-$

The C_{2v}, ($^2A_1$) structure (Fig. 5 *i*) is clearly the ground state for $YbSi_6^-$ with alternative structures being at least 0.34 eV higher in energy. The ground state of $YbSi_6^-$ is open shell ($^2A_1$) with a valence configuration of $(1a_1)^2(1b_2)^2(2a_1)^2(1b_1)^2(3a_1)^2(2b_2)^2(4a_1)^2(1a_2)^2(5a_1)^2(2b_1)^2(3b_2)^2(6a_1)^2(4b_2)^2(7a_1)^2(3b_1)^2(5b_2)^2(8a_1)^2(4b_1)^2(2a_2)^2(9a_1)^2(6b_2)^1$. Experimental photoelectron spectra of $YbSi_6^-$ generally differ from those of Ho-, Gd-, and Pr-doped $LnSi_6^-$ members, with their most characteristic distinction are being filled comparably low EBE peaks.[46] The X band in the experimental spectra is low electron binding energy peak, broad and congested, suggesting that it may contain multiple detachment channels. Indeed, the calculated VDEs for the first seven detachment channels, from the SOMO $6b_2$ (1.95 eV), $9a_1$ (1.97 eV and 1.99 eV), $2a_2$ (2.02 eV and 2.04 eV) and the $4b_1$ (2.05 eV and 2.06 eV) orbital (T and S), are very close to each other, consistent with the broad X band. The $6b_2$ SOMO is mainly a nonbonding σ orbital, as shown in Fig. 9(a) and Fig. 9(c) for the spin density. On removal of an electron, the neutral $YbSi_6$ remains the C_{2v} structure with a shorter Yb-Si bond by about 0.10~0.13 Å. The calculated VDEs from the $8a_1$ orbital, 2.62 eV(S) and 2.64 eV(T), corresponding to the removal of the spin up and spin down electrons, are in good agreement with the observed VDE of the A band (2.60±0.05 eV).[46] The simulated PES spectrum of the second lowest-energy isomer *j* present different features with that of the experimental features, suggesting structure *j* should not be a reasonable isomer. Furthermore, the theoretical first ADE/VDE (2.39/2.42 eV) values of the second lowest-energy isomer *j* agree very poorly with the experimental data (1.80±0.05/1.98 eV).[46] Overall, the simulated PES spectrum and calculated ADE/VDE from the global minimum of $YbSi_6^-$ is in very good agreement with the experimental observation (Table 3 and Fig. 5), lending considerable credence to the global minimum identified.

3.2.5. $LuSi_6^-$

The comparisons between experiment and theory for the ground state of $LuSi_6^-$ are presented in Table 3 and Fig. 6. The ground state of $LuSi_6^-$ (structure *j*) is closed shell ($^1A'$) with a valence configuration of $(1a')^2(1a'')^2(2a')^2(3a')^2(2a'')^2(4a')^2(5a')^2(6a')^2(3a'')^2(7a')^2(4a'')^2(8a')^2(5a'')^2(9a')^2$. The first calculated VDE corresponds to electron detachment from the 9a' HOMO, which is mainly a bonding σ orbital (Fig. 10(a)). The SOMO ($7a_1$) of the neutral cluster upon removing an electron from the anion HOMO is shown in Fig. 10(b) and its spin density (Fig. 10(c)) is seen to concentrate on the Lu atom. The simulated PES patterns on the basis of the two isomers (Fig. 6) appear to be rather different, the PES of the one isomer *j* is extremely loose and consists of only two bands within the 0~4.661 eV, on the contrary, the other isomer *i* presented extremely congested and consisting of five bands. For the ground state structure of $LuSi_6^-$, the calculated VDE of 3.07 eV is in good agreement with the experimental value of 3.20 eV (Table 3),[47] however, the calculated ADE of 2.86 eV is larger than the experimental value of 2.10 eV. As seen from Table 3, this situation is ambiguous when considering the first ADE. We note that the second isomer *i* is 0.35 eV above the global minimum structure, but the computed ADE (2.00 eV) agree very well with the experimental results (2.10 eV).[47] Usually it is rare to have such a high-energy isomer with coexistent in the cluster beam experiments. Considering their very close ADE, it is possible that isomer *i* is minor isomer. These results lead us to conclude that the global minimum structure *j* and minor isomer *i* might be coexistent in the $LuSi_6^-$ cluster beam.

3.3. Electronic and magnetic properties

We performed natural population analysis (NPA) for the lowest-energy structures of MSi_6^q clusters, the summarized natural charges and populations are given in Table 4. As seen from Table 4, charge always transfers from RE atom to Si atom for RE-doped MSi_6^q clusters. The transferred charges are from 0.47 *e* to 0.91 *e* for neutral MSi_6 and by 0.10 *e*~0.33 *e* for anionic species, which indicates that RE atom acts as electron donor. The Yb atom loses the largest charge (0.91 *e*) from its neighbouring Si atoms. The NPA of all the Si atoms bonding to RE atom is negative. The charge distribution is dependent on the symmetry of the cluster. Magnetic properties are one of the most interesting in cluster physics. The physicochemical property of size-selected cluster is quite different from that of single molecular or bulk material. Unfortunately, there are no Stern-Gerlach experiment for present species up to now, however, the reliability of the present DFT (PBEPBE) was validated by performing calculations on the simulated PES spectra and first ADE/VDE on pure $Si_{6/7}^-$ and many other RE-doped MSi_6^- (M=Yb, Lu, Pr, Gd, and Ho) clusters. Magnetic moment (μ_B) of 4*f*, 5*d*, 6*s*, and 6*p* states for RE atom, total magnetic moment (μ_B) of the RE atom, and total magnetic moment of the lowest-energy RE-doped MSi_6^q (M=La, Ce, Yb and Lu; q=0, –1) clusters are present in Table 5. As shown in Table 5, it can be found that the total magnetic moment of the $CeSi_6$ cluster has the largest value ($2\mu_B$) among MSi_6^q species. It can also be found that the total magnetic moments of the MSi_6^q clusters and the magnetic moments on RE do not quench when the RE is encapsulated in Si_6 outer frame structure, which is consistent with the results of the $EuSi_n$.[29] Interestingly, the total magnetic moments overwhelming majority is contributed by RE atoms. These results seem to imply that the majority of *f* electrons do not form chemical bonds between the RE atoms and their silicon cluster environment. To further understand the magnetic properties of MSi_6^q clusters, we performed a detailed analysis of the local magnetic moment of RE atom in MSi_6^q clusters. For free Yb and Lu atoms, the configurations of valence electrons are [Yb] $4f^{14}6s^2$ and [Lu] $4f$

$^{14}5d^16s^2$, which have closed 4*f* shells, primarily donate their 6*s* electrons to Si_6/Si_6^-, forming charge-transfer $YbSi_6^-/LuSi_6$ clusters with little distortions. However, for the open 4*f* shell Ce dopant, the free Ce atom with the configuration of valence electrons $4f\ ^15d^16s^2$, the 4*f* orbitals obtain electrons by 0.13 *e* for $CeSi_6$ and the electron transfer is very small for $CeSi_6^-$ from the Si_6/Si_6^- clusters.

Table 4 Natural charges populations of the lowest-energy RE-doped MSi_6^q (M=La, Ce, Yb and Lu; q=0, –1) clusters.

Cluster	Isomer	RE	Si-1	Si-2	Si-3	Si-4	Si-5	Si-6
$LaSi_6$	*i*	0.47	–0.10[a]	–0.21[a]	–0.10[a]	–0.21[a]	0.07	0.08
$LaSi_6^-$	*j*	0.16	–0.17[a]	–0.17[a]	–0.17[a]	–0.17[a]	–0.17[a]	–0.29
$CeSi_6$	*i*	0.61	–0.12[a]	–0.28[a]	–0.12[a]	–0.26[a]	0.09	0.09
$CeSi_6^-$	*j*	0.10	–0.17[a]	–0.17[a]	–0.17[a]	–0.16[a]	–0.16[a]	–0.28
$YbSi_6$	*i*	0.91	–0.21[a]	–0.34[a]	–0.21[a]	–0.34[a]	0.09	0.09
$YbSi_6^-$	*i*	0.33	–0.26[a]	–0.36[a]	–0.26[a]	–0.36[a]	–0.05	–0.05
$LuSi_6$	*i*	0.56	–0.10[a]	–0.30[a]	–0.10[a]	–0.30[a]	0.13	0.13
$LuSi_6^-$	*j*	0.30	–0.19[a]	–0.19[a]	–0.19[a]	–0.19[a]	–0.19[a]	–0.33

[a]Atoms bonding to RE atom.

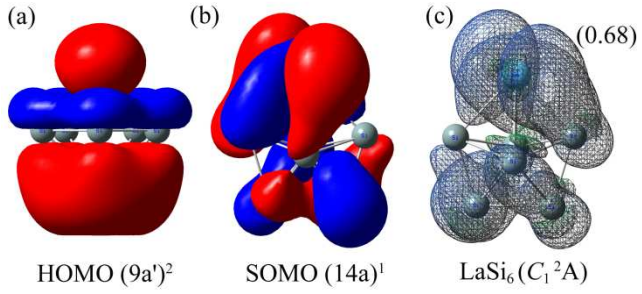

Fig. 7 (a) The HOMO picture of $LaSi_6^-$ (C_{5v}, ^{1}A'). (b) The SOMO picture of $LaSi_6$ (C_1, ^{2}A). (c) The Mülliken spin density of $LaSi_6$ (C_1, ^{2}A).

Table 5 Magnetic moment (μ_B) of 4*f*, 5*d*, 6*s*, and 6*p* states for RE atom, total magnetic moment (μ_B) of the RE atom, and total magnetic moment of the lowest-energy RE-doped MSi_6^q (M=La, Ce, Yb and Lu; q=0, –1) clusters.

Cluster	Isomer	RE Moment (μ_B)					Molecule (μ_B)
		4*f*	5*d*	6*s*	6*p*	Total	
$LaSi_6$	*i*	0.02	0.51	0.09	0.01	0.63	1
$LaSi_6^-$	*j*	0.00	0.00	0.00	0.00	0.00	0
$CeSi_6$	*i*	0.87	0.31	0.52	0.07	1.77	2
$CeSi_6^-$	*j*	1.02	0.04	0.00	0.00	1.06	1
$YbSi_6$	*i*	0.00	0.00	0.00	0.00	0.00	0
$YbSi_6^-$	*i*	0.01	0.01	0.67	0.17	0.86	1
$LuSi_6$	*i*	0.00	0.10	0.59	0.16	0.85	1
$LuSi_6^-$	*j*	0.00	0.00	0.00	0.00	0.00	0

It is interesting to describe certain trends of the magnetic moments of MSi_6^q in this work as follows: (1) Table 5 shows that $LaSi_6$, $CeSi_6^{0,-}$, $YbSi_6^-$ and $LuSi_6$ are magnetic clusters, and the magnetic moments are 1, 2, 1, 1 and 1μ_B, respectively. $LaSi_6^-$, $YbSi_6$ and $LuSi_6^-$ species present a non-magnetic ground state. (2) For all the RE-doped MSi_6^q clusters, RE atoms carry most of the magnetic moments. The magnetism of the clusters considered in this study is mainly located on the RE atoms, only very small magnetic moments are found on the parent clusters. This is quite consistent with the result of Eu doped Si clusters.[29] For $CeSi_6^-$ cluster, Si_6^- contribute small negative magnetic moment to the total moment, while for other RE-doped clusters, they carry a small positive magnetic moment. (3) The dopant RE atoms remain largely localized and the atomiclike magnetism is maintained in the doped clusters. The pure Si_6 cluster is usually non-magnetic, when being doped with different RE atoms, it sometimes becomes to be magnetic cluster.

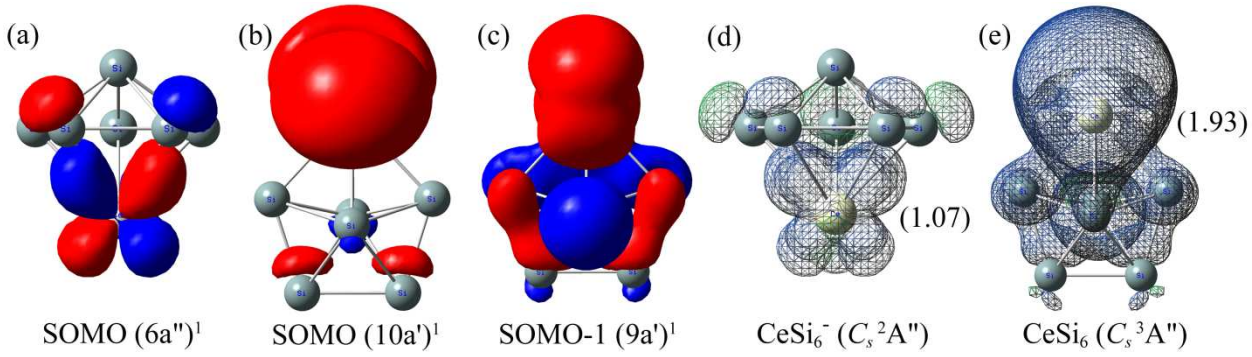

Fig. 8 (a) The SOMO picture of $CeSi_6^-$ (C_s, ^{2}A"). (b) The SOMO and (c) SOMO-1 pictures of $CeSi_6$ (C_s, ^{3}A"). (d) The Mülliken spin density of $CeSi_6^-$ (C_s, ^{2}A"). (e) The Mülliken spin density of $CeSi_6$ (C_s, ^{3}A").

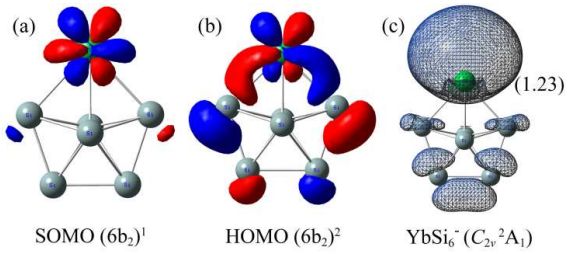

Fig. 9 (a) The SOMO picture of $YbSi_6^-$ (C_{2v}, $^2A_1$). (b) The HOMO picture of $LaSi_6$ (C_{2v}, $^1A_1$). (c) The Mülliken spin density of $YbSi_6^-$ (C_{2v}, $^2A_1$).

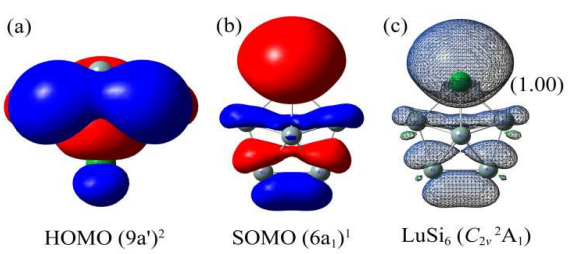

Fig. 10 (a) The HOMO picture of $LuSi_6^-$ (C_{5v}, ^{1}A'). (b) The SOMO picture of $LuSi_6$ (C_{2v}, $^2A_1$). (c) The Mülliken spin density of $LuSi_6$ (C_{2v}, $^2A_1$).

4. Conclusions

In conclusion, we have investigated the structural, electronic, and magnetic properties on a series of RE-doped neutral and charged silicon clusters MSi_6^q (M=La, Ce, Yb and Lu; q=0, –1), using former anion photoelectron spectroscopy and density-functional calculations at the PBEPBE level. Stochastic search procedure by Saunders "kick" method combined with extensive DFT calculations are used for global minimum searches (SK-DFT). Optimized geometries of the ground-state and low-lying energy states of both the anion and neutral species are reported using SK-DFT and the results are compared with experimental literature photoelectron spectroscopy results. The global minimum search revealed that the MSi_6^- (M= La, Ce, and Lu) is a three-dimensional structure with the lanthanide-metal atom sitting on top (or bottom) of the regular pentagonal bipyramid, which is obtained by substituting one Si by M atom from the bottom (or top) of the pure $Si_7^{-,0}$ cluster. Instead, the neutral species and $YbSi_6^-$ show the impurity as a four-coordinate atom in the equatorial plane of pentagonal bipyramid, which obtained by substituting one Si in the equatorial plane by M atom from the ground state structure of Si_7 cluster. The $CeSi_6^{-,0}$ clusters have the largest binding energy and doping energy, indicating that the neutral and anionic $CeSi_6$ clusters should be the most stable among MSi_6^q species. The study of magnetic property indicates that the magnetic moment of the doped RE atoms remain largely localized and the atomiclike magnetism is maintained in the doped clusters. The pure Si_6 cluster is usually non-magnetic, when being doped with different RE atoms, it sometimes becomes to be magnetic cluster. The current Si_6 doping with different RE atoms suggest that a new class of pentagonal bipyramid clusters with varying magnetic properties may exist. The systematic methods, including structural characteristic and magnetic property, presented in this study are useful for the analysis of the theoretical and experimental data and provide insight into more complicated cluster systems.

Acknowledgements

This work was supported by the Natural Science Foundation of Fujian Province of China (No. 2012J05005), by the Program for Excellent Youth Talents in Universities of Fujian Province of China (No. JA13009), and by the Fundamental Research Funds for the Central Universities (JB-ZR1201).

Notes and references

College of Engineering, Huaqiao University, Quanzhou, 362021, China. Email: hqwang@hqu.edu.cn

1 W. L. Brown, R. R. Freeman, K. Raghavachari and M. Schlueter, *Science*, 1987, **235**, 860.
2 J. T. Lyon, P. Gruene, A. Fielicke, G. Meijer, E. Janssens, P. Claes and P. Lievens, *J. Am. Chem. Soc*., 2009, **131**, 1115.
3 M. Haertelt, J. T. Lyon, P. Claes, J. Haeck, P. Lievens and A. Fielicke, *J. Chem. Phys*., 2012, **136**, 064301.
4 S. J. Peppernick, K. D. D. Gunaratne, S. G. Sayres and A. W. Castleman, Jr., *J. Chem. Phys*., 2010, **132**, 044302.
5 W. A. Tiznado, P. Fuentealba and J. V. Ortiz, *J. Chem. Phys*., 2005, **123**, 144314.
6 C. Xu, T. R. Taylor, G. R. Burton and D. M. Neumark, *J. Chem. Phys*., 1998, **108**, 1395.
7 K.-H. Ho, A. A. Shvartsburg, B. Pan, Z. Y. Lu, C. Z. Wang, J. G. Wacker, J. L. Fye and M. F. Jarrold, *Nature*, 1998, **392**, 582.
8 A. Tekin and B. Hartke, *Phys. Chem. Chem. Phys*., 2004, **6**, 503.
9 O. Lehtonen and D. Sundholm, *Phys. Chem. Chem. Phys*., 2006, **8**, 4228.
10 X. Chu, M. Yang and K. A. Jackson, *J. Chem. Phys*., 2011, **134**, 234505.
11 R. L. Zhou and B. C. Pan, *J. Chem. Phys*., 2008, **128**, 234302.
12 C. Pouchan, D. Bégué and D. Y. Zhang, *J. Chem. Phys*., 2004, **121**, 4628.
13 R. R. Hudgins, M. Imai, M. F. Jarrold and P. Dugourd, *J. Chem. Phys*., 1999, **111**, 7865.
14 S. M. Beck, *J. Chem. Phys*., 1989, **90**, 6306.
15 P. Claes, V. T. Ngan, M. Haertelt, J. T. Lyon, A. Fielicke, M. T. Nguyen, P. Lievens and E. Janssens, *J. Chem. Phys*., 2013, **138**, 194301.
16 J.T. Lau, K. Hirsch, Ph. Klar, A. Langenberg, F. Lofink, R. Richter, J. Rittmann, M. Vogel, V. Zamudio-Bayer, T. Möller and B. v. Issendorff, *Phys. Rev. A*, 2009, **79**, 053201.
17 A. Grubisic, H. Wang, Y. J. Ko and K. H. Bowen, *J. Chem. Phys*., 2008, **129**, 054302.
18 E. Janssens, P. Gruene, G. Meijer, L. Wöste, P. Lievens and A. Fielicke, *Phys. Rev. Lett*., 2007, **99**, 063401.
19 K. Koyasu, J. Atobe, M. Akutsu, M. Mitsui and A. Nakajima, *J. Phys. Chem. A*, 2007, **111**, 42.
20 K. Koyasu, M. Akutsu, M. Mitsui and A. Nakajima, *J. Am. Chem. Soc*., 2005, **127**, 4998.
21 M. Ohara, K. Koyasu, A. Nakajima and K. Kaya, *Chem. Phys. Lett*., 2003, **371**, 490.
22 M. Ohara, K. Miyajima, A. Pramann, A. Nakajima and K. Kaya, *J. Phys. Chem. A*, 2002, **106**, 3702.
23 H. Hiura, T. Miyazaki and T. Kanayama, *Phys. Rev. Lett*., 2001, **86**, 1733.
24 N. M. Tam, T. B. Tai, V. T. Ngan and M. T. Nguyen, *J. Phys. Chem. A*, 2013, **117**, 6867.
25 S. Jaiswal, V. P. Babar and V. Kumar, *Phys. Rev. B*, 2013, **88**, 085412.
26 L. Guo, X. Zheng, Z. Zeng and C. Zhang, *Chem. Phys. Lett*., 2012, **550**, 134.
27 H. Cantera-López, L. C. Balbás and G. Borstel, *Phys. Rev. B*, 2011, **83**, 075434.
28 R. N. Zhao, J. G. Han, J. T. Bai, F. Y. Liu and L. S. Sheng, *Chem. Phys*., 2010, **372**, 89.
29 G. F. Zhao, J. M. Sun, Y. Z. Gu and Y. X. Wang, *J. Chem. Phys*., 2009, **131**, 114312.
30 R. N. Zhao, Z. Y. Ren, P. Guo, J. T. Bai, C. H. Zhang and J. G. Han, J. Phys. Chem. *A*, 2006, **110**, 4071.
31 P. Guo, Z. Y. Ren, A. P. Yang, J. G. Han, J. Bian and G. H. Wang, *J. Phys. Chem. A*, 2006, **110**, 7453.
32 J. G. Han, Z. Y. Ren and B. Z. Lu, *J. Phys. Chem. A*, 2004, **108**, 5100.
33 V. Kumar, A. K. Singh and Y. Kawazoe, *Nano Lett*., 2004, **4**, 677.
34 J. Lu and S. Nagase, *Phys. Rev. Lett*., 2003, **90**, 115506.
35 H. F. Li, X. Y. Kuang and H. Q. Wang, *Phys. Lett. A*, 2011, **375**, 2836.
36 R. N. Zhao, J. G. Han, J. T. Bai, F. Y. Liu and L. S. Sheng, *Chem. Phys*., 2010, **378**, 82.
37 T. T. Cao, X. J. Feng, L. X. Zhao, X. Liang, Y. M. Lei and Y. H. Luo, *Eur. Phys. J. D*, 2008, **49**, 343.
38 H. Bai, H. J. Zhai, S. D. Li and L. S. Wang, *Phys. Chem. Chem. Phys*., 2013, **15**, 9646.
39 W. L. Li, C. Romanescu, Z. A. Piazza and L. S. Wang, *Phys. Chem. Chem. Phys*., 2012, **14**, 13663.
40 T. R. Galeev, A. S. Ivanov, C. Romanescu, W. L. Li, K. V. Bozhenko, L. S. Wang and A. I. Boldyrev, *Phys. Chem. Chem. Phys*., 2011, **13**, 8805.
41 H. J Zhai, W. J. Chen, X. Huang and L. S. Wang, *RSC Adv*., 2012, 2, 2707.
42 H. T. Liu, Y. L. Wang, X. G. Xiong, P. D. Dau, Z. A. Piazza, D. L. Huang, C.-Q. Xu, J. Li and L. S. Wang, *Chem. Sci*., 2012, **3**, 3286.
43 R. Pal, L. M. Wang, W. Huang, L. S. Wang and X.C. Zeng, *J. Am.*

Chem. Soc., 2009, **131**, 3396.
44 H. J. Zhai, B. Wang, X. Huang and L. S. Wang, *J. Phys. Chem. A*, 2009, **113**, 3866.
45 H. J. Zhai, B. B. Averkiev, D.Yu. Zubarev, L. S. Wang and A.I. Boldyrev, *Angew. Chem., Int. Ed*., 2007, **46**, 4277.
46 A. Grubisic, Y. J. Ko, H. Wang and K. H. Bowen, *J. Am. Chem. Soc*., 2009, **131**, 10783.
47 K. Koyasu, J. Atobe, S. Furuse and A. Nakajima, *J. Chem. Phys*., 2008, **129**, 214301.
48 M. Saunders, *J. Comput. Chem*., 2004, **25**, 621.
49 J. P. Perdew, K. Burke and M. Ernzerhof, *Phys. Rev. Lett*., 1996, **77**, 3865.
50 M. J. Frisch *et al*., GAUSSIAN09, Revision C.01, Gaussian, Inc., Wallingford, CT, 2010.
51 H. F. Li and H. Q. Wang, *Phys. Chem. Chem. Phys*., 2014, **16**, 244.
52 H. Q. Wang, H. F. Li and X. Y. Kuang, *Phys. Chem. Chem. Phys*., 2012, **14**, 5272.
53 H. Q. Wang and H. F. Li, *J. Chem. Phys*., 2012, **137**, 164304.
54 H. Q. Wang and H. F. Li, *Chem. Phys. Lett*., 2012, **554**, 231.
55 H. Q. Wang, H. F. Li, J. X. Wang and X. Y. Kuang, *J. Mol. Model*., 2012, **18**, 2993.
56 H. Q. Wang and H. F. Li, *Comput. Theor. Chem*., 2013, **1006**, 70.
57 H. Q. Wang, H. F. Li and L. X. Zheng, *J. Magn. Magn. Mater*., 2013, **344**, 79.
58 X. Cao and M. Dolg, *J. Mol. Struct. Theochem*., 2002, **581**, 139.
59 M. Dolg, H. Stoll and H. Preuss, *J. Chem. Phys*., 1989, **90**, 1730.
60 C. Paduani and P. Jena, *J. Nano. Res*., 2012, **14**, 1035.
61 A. D. Becke, *Phys. Rev. A*, 1988, **38**, 3098.
62 J. P. Perdew and Y. Wang, *Phys. Rev. B*, 1992, **45**, 13244.
63 A. D. Becke, *J. Chem. Phys*., 1993, **98**, 5648.
64 C. Lee, W. Yang and R. G. Parr, *Phys. Rev. B*, 1988, **37**, 785.
65 B. Mielich, A. Savin, H. Stoll and H. Preuss, *Chem. Phys. Lett*., 1989, **157**, 200.
66 D. J. Tozer and N. C. Handy, *J. Chem. Phys*., 1998, **109**, 10180.
67 S. F. Li and X. G. Gong, *J. Chem. Phys*., 2005, **122**, 174311.